Inhibition of Armco iron corrosion in 1 M HCl medium using saponin: Experimental and computational studies

M. Şahin,[1] S. Bilgiç[2]* and G. Gece[3]

[1]*Department of Energy Systems Engineering, Faculty of Engineering and Natural Sciences, Yıldırım Beyazıt University, Ankara 06050, Turkey*
[2]*Department of Chemistry, Faculty of Science, Ankara University, Ankara 06100, Turkey*
[3]*Department of Chemistry, Faculty of Engineering and Natural Sciences, Bursa Technical University, Bursa 16310, Turkey*
**E-mail: bilgic@science.ankara.edu.tr*

Abstract

There is a dire need in recent years for new eco-friendly compounds to combat the threat of metal corrosion. For this purpose, the present work was devoted to testing the saponin extracted from *Gypsophila simonii* plant which is a native species in Turkey as a corrosion inhibitor for Armco iron in 1 M HCl solution through Tafel extrapolation and linear polarization techniques, as well as theoretical approach for the evaluation of the inhibition efficiency at different temperatures. Corrosion current densities, percentage inhibition efficiencies, and surface coverage degrees have been determined. The results obtained showed that when the concentrations of saponin increased, corrosion rates decreased at all temperatures studied. However, the increase in temperatures resulted in a decrease in inhibition efficiency. It has been determined that saponin prevents the corrosion due to adsorption on the iron surface and obeys Langmuir isotherm, which has also been borne out by scanning electron microscopy and density functional theory studies.

Keywords: *corrosion inhibition, Armco iron, saponin, DFT.*

Received: September 16, 2020. Published: November 20, 2020 doi: 10.17675/2305-6894-2020-9-4-16

1. Introduction

Iron is typically the favored material in many major fields such as infrastructure, transportation, energy, manufacturing, public utilities, *etc*. However, it is susceptible to corrosion, both externally and internally, causing a huge concern for the industry [1, 2]. From classical anodizing inhibitors such as chromates and nitrites to latest classes of deemed nontoxic organic chemicals [3], every conceivable aspect in the quest to reduce corrosion process of metals is being explored anew through the use of multifarious corrosion inhibitors [4, 5]. Due to the current general attitude toward problems of environmental pollution, inhibitors that have the characteristics of non-poisonous substances, and whose disbursement is sufficiently low to permit widespread application, are of special interest [6, 7]. Although there are a large number of studies about the inhibition effect of various compounds on the

corrosion of iron in HCl environment [8–10], the number of studies with plant extracts on the corrosion of pure iron in an acidic environment are almost nonexistent [11, 12].

In this regard, there is a compelling reason for interest in the study of saponins since they have been reported to be present in more than 100 families of plants and in a few marine sources such as star fish and sea cucumber, and also they have a diverse range of properties such as pharmacological, medicinal, hemolytic, as well as antimicrobial, insecticidal, and molluscicidal activities which make them eligible as corrosion inhibitors due to their intrinsic structural propinquity [13–15]. Saponins are secondary plant compounds with a rigid skeleton of at least four hydrocarbon rings to which sugars in groups of one or two are attached, and the variety of glycones, carbohydrates, and different attachment positions result in numerous types of saponins.

Accordingly, it is apt in this context to clarify the question of whether saponins can account for the inhibition of iron corrosion in aggressive media. To this end, the inhibitory effect of saponin (Figure 1) obtained by extraction from the roots of *Gypsophila simonii* plant which is a native species in Turkey [16] on the corrosion of iron in 1 M HCl environment was investigated. For determination of corrosion parameters at several concentrations and temperatures, Tafel extrapolation and linear polarization methods have been used. The relationship between the structure and inhibition performance of saponin has also been revealed by theoretical calculations [17–19].

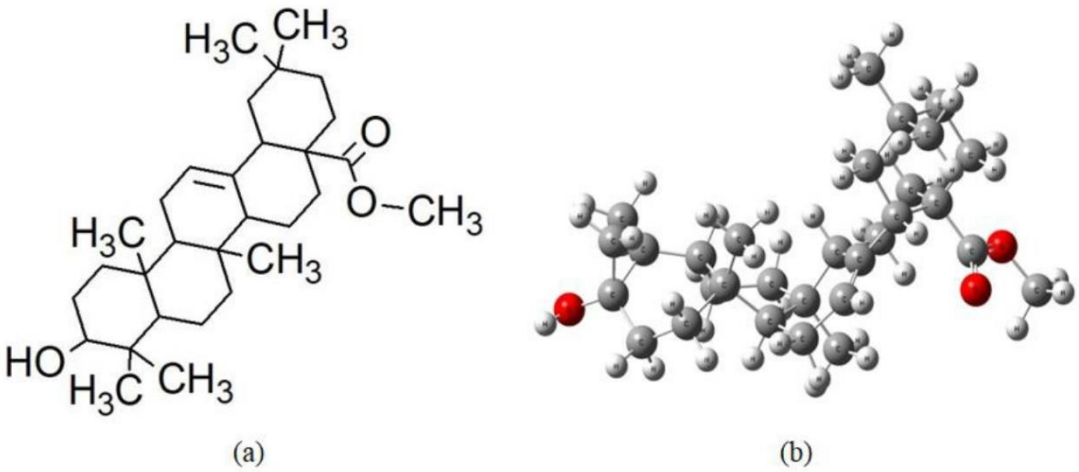

Figure 1. (a) Molecular and (b) optimized structure of the studied gypsogenin ester saponin in aqueous phase at M06-2X/DGDZVP level.

2. Experimental and Theoretical Details

Electrochemical experiments were performed using a conventional three electrode cell assembly. The working electrode was an Armco iron with a diameter of 4 mm which was made cylindrical and embedded in methyl acrylate, and has the following composition (wt. %): 0.0013–0.0060 C, 0.00–0.03 Si, 0.06–0.10 Mn, 0.02–0.32 S, 0.05–0.07 P, and the

balance is Fe. A silver/silver chloride (Ag/AgCl) electrode and Pt electrode were used as the reference electrode and auxiliary electrode, respectively. All the measured potentials presented in this paper are referred to Ag/AgCl electrode. Pre-treatment of the iron electrode was carried out by abrading with emery paper of 1200 grit and polishing with 0.5 μm alumina, rinsing with bi-distilled water, and then immersing into the cell. All of the test solutions were prepared using bidistilled water and deaerated with N_2 for about 20–25 min before each experiment to remove the dissolved O_2 in the solution. During the experiments, the solution was mixed with a magnetic stirrer. The experiments were implemented with 100, 200, 300, 400, and 500 ppm concentrations of saponin at 298, 308, 318, 328, and 338 K temperatures. In experiments at different temperatures, the temperature was controlled by circulation in a water bath. Corrosion parameters were assessed with CHI Electrochemical Analyzer by the obtained polarization curves recorded at the scan rate of 2.5 mV/s.

Saponin molecule was built and optimized to a minimum using Gaussian09 program package [20]. The geometry optimization was achieved using the exchange–correlation functional, M06-2X due to its good performance on ionization potentials and electron affinities, as well as dispersion-like interactions [21]. In addition, the double-zeta basis set, DGDZVP was applied in order to include an all-electron description of the different atoms present in the studied compound. The gas-phase optimized geometry was obtained with the level of theory, M06-2X/DGDZVP. This structure was reoptimized in the presence of water as implicit solvent; in this case, the continuum solvation model SMD was used [22]. The effects of the frontier molecular orbital energies, their differences, and some reactivity parameters were investigated.

3. Results and Discussion

The obtained Tafel curves of iron in 1 M HCl and in the presence of various concentrations of saponin are shown in Figure 2. The corrosion potentials (E_{corr}) determined from curves, anodic and cathodic Tafel slopes (β_a and β_c), corrosion current density (i_{corr}), degree of surface coverage (θ), and percentage inhibition efficiency (η%) are given in Table 1. Surface coverage ratio (θ) and inhibition efficiency values (η%) were calculated from the following equations:

$$\theta = \frac{i_{corr} - i'_{corr}}{i_{corr}} \quad (1)$$

$$\eta\% = \frac{i_{corr} - i'_{corr}}{i_{corr}} \times 100 \quad (2)$$

where i_{corr} and i'_{corr} are the values of the corrosion current density of uninhibited and inhibited solutions, respectively. As can be seen from Figure 2 and Table 1, with increasing saponin concentrations, the corrosion potential shifts to positive, while the anodic and cathodic Tafel slopes do not show a systematic change, however, the corrosion currents decrease. The inhibition efficiencies and the degree of surface coverage also increase depending on the

concentrations. By increasing the temperature for the same inhibitor concentrations, corrosion current densities increase and inhibition activities decrease.

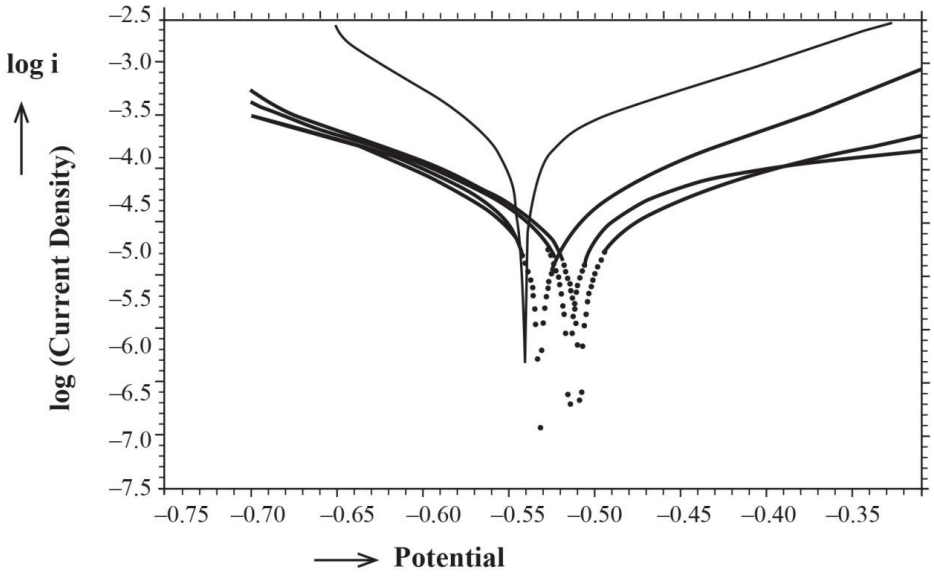

Figure 2. Tafel curves of iron in 1 M HCl (—), and in the presence of 100 ppm (♦), 200 ppm (o), 400 ppm (•) saponin.

Table 1. Corrosion parameters for iron in 1 M HCl in the absence and presence of saponin at different temperatures.

Temperature, K	Concentration, ppm	$-E_{corr}$, mV	i_{corr}, μA·cm^{-2}	β_a, mV·dec^{-1}	β_c, mV·dec^{-1}	η, %	θ
298	No inhibitor	536	468.1	123	112	–	–
	100	526	143.2	128	132	69.4	0.694
	200	514	87.9	136	127	81.2	0.812
	300	505	59.5	131	146	87.3	0.873
	400	492	40.2	143	135	91.4	0.914
	500	487	31.9	140	148	93.2	0.932
308	No inhibitor	529	792.4	110	99	–	–
	100	520	252.7	116	102	68.1	0.081
	200	518	164.3	123	105	79.3	0.793
	300	508	115.7	119	111	85.4	0.854
	400	502	86.3	126	106	89.1	0.891
	500	493	68.2	135	119	91.4	0.914

Temperature, K	Concentration, ppm	$-E_{corr}$, mV	i_{corr}, μA·cm^{-2}	β_a, mV·dec^{-1}	β_c, mV·dec^{-1}	η, %	θ
318	No inhibitor	531	1346.1	114	96	–	–
	100	527	523.6	112	105	61.1	0.611
	200	519	399.7	106	103	70.3	0.703
	300	510	274.6	110	111	79.6	0.796
	400	503	187.1	123	116	86.1	0.861
	500	498	152.1	128	121	88.7	0.887
328	No inhibitor	527	1887.5	108	90	–	–
	100	516	826.5	101	89	56.2	0.562
	200	520	690.8	109	105	63.4	0.634
	300	510	585.1	121	107	69.6	0.696
	400	503	394.5	111	110	79.1	0.791
	500	490	318.9	114	108	83.1	0.831
338	No inhibitor	530	2343.6	100	86	–	–
	100	519	1352.3	96	89	42.3	0.423
	200	522	1005.4	111	94	57.1	0.571
	300	511	843.5	109	96	64.0	0.640
	400	500	749.7	121	110	68.4	0.684
	500	496	562.3	119	111	76.6	0.766

Another method to determine the corrosion rate, *i.e.*, i_{corr} values, is the linear polarization or polarization resistance method. Theoretical foundations of the method were given by Stern and Geary [23]. According to Stern and Geary, there is a linear relationship between potential and current at potentials slightly shifted away from the corrosion potential E_{corr}. This linear relation can only be applied between certain values. An equation has been derived which relates the slope of a polarization curve in the vicinity of the corrosion potential to the corrosion current density i_{corr}. The Stern–Geary equation is expressed as $i_{corr} = B\Delta I/\Delta E$, where B is a constant determined by anodic and cathodic Tafel slopes β_a and β_c by Equation 3 and, R_p is called polarization resistance which can be measured as by Equation 4 in a polarization test.

$$i_{corr} = \frac{\beta_a \beta_c}{2.303(\beta_a + \beta_c)R_p} \quad (3)$$

$$R_p = \frac{\Delta E}{\Delta I} \quad (4)$$

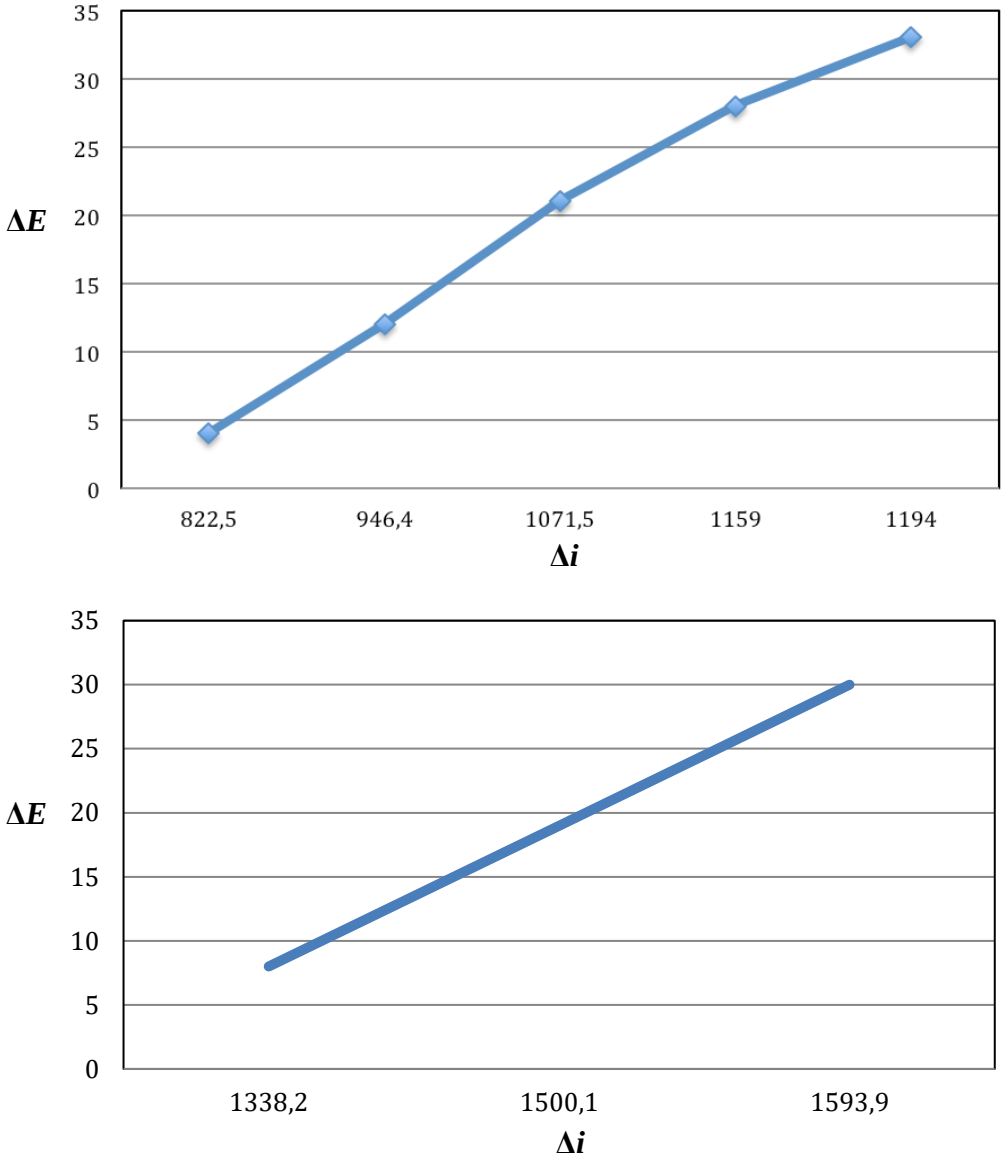

Figure 3. Stearn–Geary graph at (a) 318 K and (b) 338 K.

In the Equation 4, Δ*E* is the amplitude of the potential shift away from E_{corr} and Δ*i* is the measured change of current corresponding to Δ*E* (Figure 3). Thus, corrosion rates were determined by linear polarization method and the results were compared with those of Tafel extrapolation in Table 2. In this table, percentage inhibition efficiency (η%) values determined by linear polarization method are also listed. As can be seen from the tables when the concentrations of the inhibitor increase potentials shift to more anodic values, corrosion rates reduce and the inhibition efficiencies and surface coverage degrees increase. According to Bockris and Drazic [24], the inhibition mechanism can be explained by the $Fe(Inh)_{ads}$ reaction intermediates:

$$Fe + Inh \leftrightarrow Fe(Inh)_{ads} \leftrightarrow Fe^{n+} + ne^{-} + Inh$$

At first, when there is no enough $Fe(Inh)_{ads}$ to cover the metal surface because the inhibitor concentration is either low or the adsorption rate is slow, metal dissolution takes place on sites on the iron surface free of $Fe(Inh)_{ads}$. With high inhibitor concentration, a compact and coherent inhibitor over layer is formed on iron that reduces chemical attacks on the metal. The protective effects of inhibitors on the metal surfaces are often explained through adsorption isotherms. The adsorption of inhibitor molecules from aqueous solutions can be regarded as a quasi-substitution process between the organic compound in the aqueous phase $Org_{(aq)}$ and water molecules at the electrode surface, $H_2O_{(s)}$:

$$Org_{(aq)} + xH_2O_{(s)} \rightleftarrows Org_{(s)} + xH_2O_{(aq)} \quad (5)$$

where x is the size ratio, that is, the number of water molecules replaced by one organic inhibitor. Adsorption isotherms are very important in determining the mechanism of organo-electrochemical reactions [25]. The most frequently used isotherms are Henry, Langmuir, Frumkin, Hill de Boer, Parsons, Temkin, Freundlich, Flory–Huggin, Dhar-Flory Huggins, and Bockris-Swinkels [26]. All these isotherms are of the general form of the adsorption

$$f(\theta, x)\exp(-2a\theta) = KC \quad (6)$$

where $f(\theta,x)$ is the configurational factor which depends upon the physical model and the assumptions underlying the derivation of the isotherm, θ is the surface coverage degree, C is the inhibitor concentration in the electrolyte, x is the size factor ratio, a is the molecular interaction parameter, and K is the equilibrium constant of the adsorption process. When the change of surface coverage degree (θ) with the concentration of saponin (C) was examined, it was determined that the adsorption on the surface fits the Langmuir isotherm for each temperature (Figure 4).

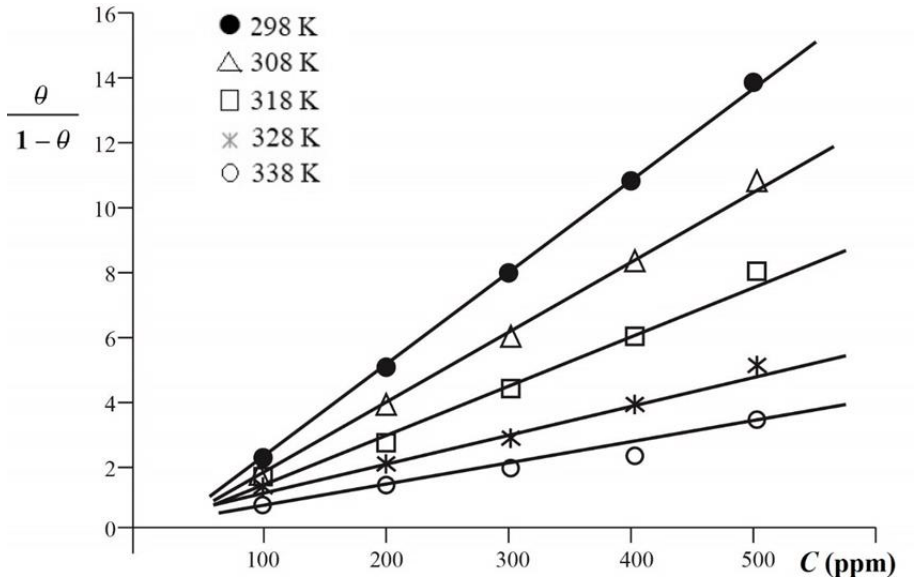

Figure 4. Langmuir adsorption isotherm plots for corrosion of iron in 1 M HCl at different concentrations of saponin.

Langmuir isotherm is given as below

$$\frac{\theta}{1-\theta} = KC \tag{7}$$

where K is adsorption equilibrium constant, and varies with adsorption free energy ΔG^0_{ads} according to Equation 8.

$$K = \frac{1}{55.5}\exp\left(\frac{-\Delta G^0_{\text{ads}}}{RT}\right) \tag{8}$$

Moreover, the Gibbs-Helmholtz equation is as below:

$$\left[\frac{\partial\left(\frac{\Delta G}{T}\right)}{\partial T}\right] = -\frac{\Delta H}{T^2}(P = \text{const}) \tag{9}$$

Then, in order to create a function relating free energy to temperature, Equation 10 should be solved.

$$\Delta G = -T\int\frac{\Delta H(T)}{T^2}dT \tag{10}$$

From Equation 10, the following equation can be written:

$$\frac{\Delta G}{T} = \frac{\Delta H}{T} + K \tag{11}$$

As can be seen in Figure 5, a straight line with an inclination almost zero and parallel to the abscissa is obtained by the variation of $\frac{\Delta G}{T}$ with $\frac{1}{T}$. Inhibitor adsorption on iron surface is more effective at low temperatures. The decrease of inhibition can be attributed to the increase of desorption with increasing temperature. Saponin, which is adsorbed as a monolayer on the surface with low temperature, is more desorbed with the increase of temperature and its inhibition efficiency decreases. As can be seen from Table 2, the inhibition performance and adsorption is more effective at lower temperatures for the saponin concentrations. This situation is explained by Labjar *et al.* [27]. They suggested that elevated temperature causes a decrease in the strength of the adsorption process. The decrease in adsorption strength characterized the physical adsorption type. At high temperature, the inhibitor molecules and particles in the bulk solution move vigorously. For this reason, inhibitor molecules are unable to adsorb permanently on the iron surface due to continuous collisions of all particles in the solution. Our experimental results are also in accordance with other literature findings [28–30]. The SEM was performed to further get the information of corrosion process. Figure 6 shows an SEM image of iron exposed to a 1 M HCl solution after immersing with and without saponin. The SEM morphology of iron

before immersion in corrosive solution showed a freshly polished metal surface (Figure 6a). As shown in Figure 6b, the surface of iron without saponin was severely corroded and some corrosion pitting appears. The SEM images of iron specimens after immersing in acid with saponin are shown in Figure 6c, the rate of corrosion was suppressed, and the corrosion pitting was significantly reduced. Comparing the two illustrations in Figures 6b and 6c, it can be concluded that Figure 6c shows smoother surface with saponin-inhibited iron corrosion.

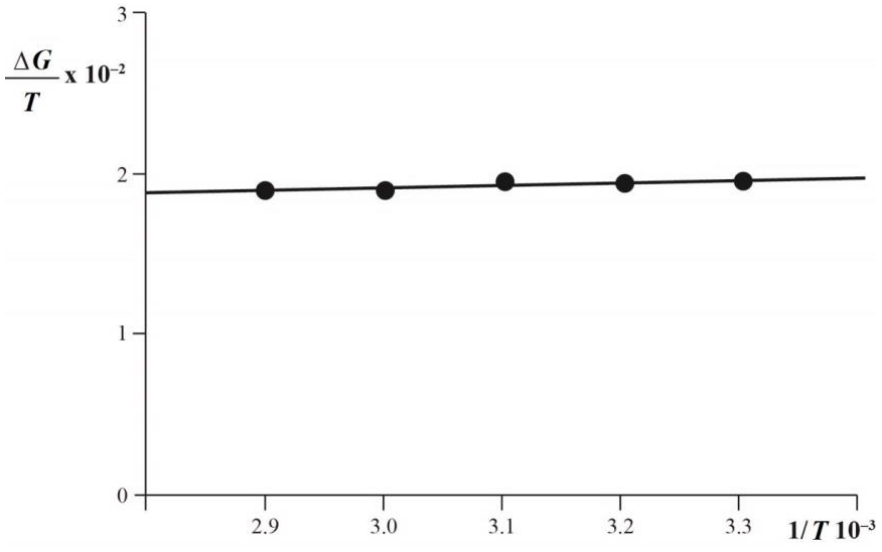

Figure 5. The variation of $\frac{\Delta G}{T}$ with $\frac{1}{T}$.

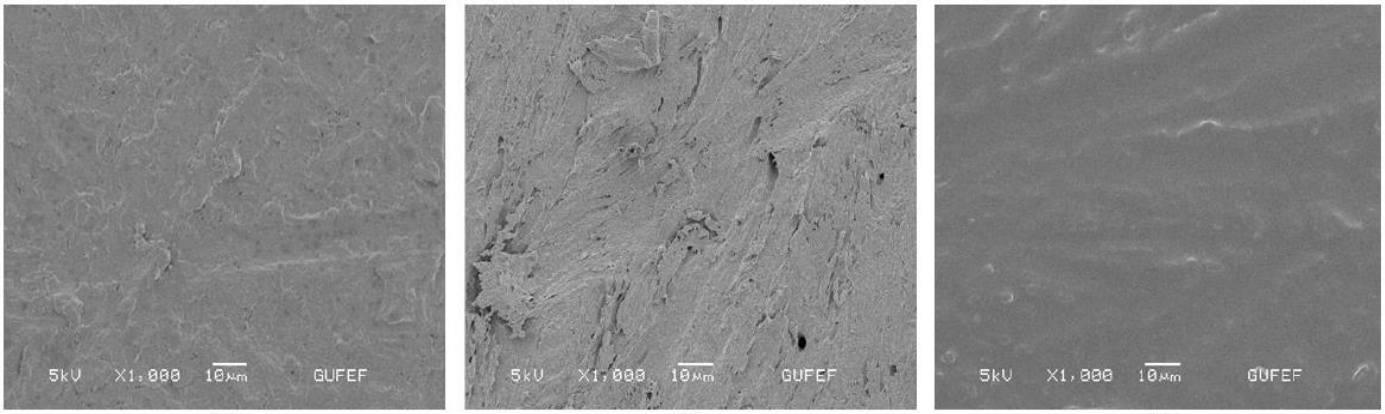

Figure 6. SEM morphology of iron specimens: (a) only polished surface, (b) immersed in 1 M HCl, and (c) in the presence of saponin.

Table 2. Corrosion parameters obtained from Tafel extrapolation and linear polarization methods for iron in 1 M HCl in the absence and presence of saponin at different temperatures.

Temperature, K	Concentration, ppm	$-E_{corr}$, mV	Tafel extrapolation		Linear polarization	
			i_{corr}, μA·cm^{-2}	η, %	R_p, Ω·cm^{-2}	η, %
298	No inhibitor	536	468.1	–	38.3	–
	100	526	143.2	69.4	118.7	68.1
	200	514	87.9	81.2	192.4	80.3
	300	505	59.5	87.3	271.6	85.9
	400	492	40.2	91.4	379.0	89.9
	500	487	31.9	93.2	461.4	91.7
308	No inhibitor	529	792.4	–	26.1	–
	100	520	252.7	68.1	79.1	67.3
	200	518	164.3	79.3	118.6	78.1
	300	508	115.7	85.4	163.1	84.6
	400	502	86.3	89.1	271.5	88.7
	500	493	68.2	91.4	290.0	91.0
318	No inhibitor	531	1346.1	–	17.6	–
	100	527	523.6	61.1	45.0	60.8
	200	519	399.7	70.3	57.9	69.6
	300	510	274.6	79.6	93.4	76.4
	400	503	187.1	86.1	117.2	85.1
	500	498	152.1	88.7	135.4	87.3
328	No inhibitor	527	1887.5	–	11.9	–
	100	516	826.5	56.2	36.4	55.4
	200	520	690.8	63.4	51.3	62.2
	300	510	585.1	69.6	56.1	67.3
	400	503	394.5	79.1	65.6	78.1
	500	490	318.9	83.1	68.4	82.6
338	No inhibitor	530	2343.6	–	5.6	–
	100	519	1352.3	42.3	9.3	42.1
	200	522	1005.4	57.1	12.7	56.8
	300	511	843.5	64.0	15.1	63.1
	400	500	749.7	68.4	16.9	66.9
	500	496	562.3	76.6	31.5	74.6

The electronic properties of saponin, effects of the frontier molecular orbital energies, the differences between lowest unoccupied molecular orbital (LUMO) and highest occupied molecular orbital (HOMO) energies ($\Delta E = E_{LUMO} - E_{HOMO}$), and dipole moment ($\mathcal{d}$) as an indicator of the electronic distribution in a molecule were investigated. Following Koopmans' theorem, several intrinsic molecular quantities like electronegativity (χ, a measure of the power of a group of atoms to attract electrons towards itself), global hardness (η, a parameter related to the resistance of an atom to a charge transfer) and global softness (σ, which shows the reactivity of the inhibitor molecules in terms of charge transfer), electrophilicity (ω, a descriptor of reactivity that allows a quantitative classification of the global electrophilic nature of a molecule within a relative scale and is effectively the power of a system to soak up electrons), which are supposed to influence the overall reaction between saponin and iron surface, have been calculated [31]. The ionization potential (I) and electron affinity (A) are interpreted as $I = -E_{HOMO}$ and $A = -E_{LUMO}$. In numerical applications, chemical potential μ and hardness η are expressed on the basis of finite difference approximations in terms of I and A. Following equations: $\chi = (I+A)/2 = -\mu$; $\eta = (I-A)/2$; $S = (2\eta)^{-1}$; and $\omega = \mu^2/2\eta$ are used for the calculation of the absolute electronegativity, χ, the absolute hardness, η, the global chemical softness, S, and electrophilicity index, ω, respectively. The fraction of electrons transferred (ΔN) is also calculated by $\Delta N = (\chi_{Fe} - \chi_{sap})/2(\eta_{Fe} - \eta_{sap})$, where experimental polycrystalline work function value of bulk iron, $\chi_{Fe} = 4.5$ eV [32], and a global hardness of $\eta_{Fe} = 0$ eV were used based on the assumption that for a bulk metal $I = A$ because they are softer than the neutral metallic atoms. The main idea underlying this equation is not quantities of transferred electron from donor centers to acceptor centers and the ΔN values only shows trend [33]. The computed parameters are presented in Table 3. The theoretical data in this table show that saponin has the highest E_{HOMO} and the lowest E_{LUMO} and ΔE values in aqueous phase rather than gas phase. A more reactive nucleophile is characterized by a lower value of ω, in opposite a good electrophile is characterized by a high value of ω. In this regard, saponin seems to behave as a nucleophile in aqueous phase. A hard molecule has a large energy disparity and a soft molecule has a small energy disparity. Soft molecules are more reactive than hard ones because they could easily offer electrons to an acceptor. As is seen, the values of η and S for saponin do not differ from each other in both phases. The higher value of $\mathcal{d}$ for saponin in aqueous phase corresponds to the higher inhibition efficiency of this compound in corrosive medium as compared to that in the gas phase. If $\Delta N < 3.6$, the inhibition efficiency enhances with increasing electron-donating ability to the metal surface. As shown in Table 3, the negative sign of calculated ΔN values in both phases indicates that electrons are transferred from iron surface to saponin.

Table 3. Quantum chemical parameters of the studied saponin.

Parameters	Phase[a]	Saponin
E_{HOMO}, eV	G	−7.628
	A	−7.553
E_{LUMO}, eV	G	1.179
	A	1.057
ΔE ($E_{LUMO}-E_{HOMO}$), eV	G	8.807
	A	8.610
∂ (D)	G	0.801
	A	1.833
ω	G	1.181
	A	1.225
χ	G	3.225
	A	3.248
η	G	4.404
	A	4.305
S	G	0.155
	A	0.154
ΔN	G	−0.145
	A	−0.145

[a] G, gas phase (ε = 1.0); A, aqueous phase (ε = 78.5).

4. Conclusions

The adsorption behavior and anti-corrosion potential of saponin towards iron in 1 M HCl were investigated. The main conclusions of our work are summarized below.

- The adsorption of saponin on the iron surface fits the Langmuir isotherm at all temperatures.
- The inhibition efficiency of saponin decreases with increasing temperature.
- The highest inhibition occurs at 298 K at a concentration of 500 ppm saponin.
- Theoretical study also confirms the inhibitory action of saponin by adsorption.

Acknowledgments

The authors are grateful to Prof. Dr. Levent Aksu and Prof. Dr. Demet Çetin (Gazi University) for their technical support.

References

1. C. Verma, J. Haque, M.A. Quraishi and E.E. Ebenso, Aqueous phase environmental friendly organic corrosion inhibitors derived from one step multicomponent reactions: a review, *J. Mol. Liq.*, 2019, **275**, 18–40. doi: 10.1016/j.molliq.2018.11.040
2. F.O. Edoziuno, A.A. Adediran, B.U. Odoni, M. Oki and O.S. Adesina, Comparative analysis of corrosion inhibition effects of mebendazole (MBZ) on mild steel in three different sulphuric acid concentrations, *Int. J. Corros. Scale Inhib.*, 2020, **9**, no. 3, 1049–1058. doi: 10.17675/2305-6894-2020-9-3-17
3. C. Monticelli, *Encyclopedia of Interfacial Chemistry*, ed. K. Wandelt, Elsevier, Amsterdam, 2018, 164.
4. Y. Zhu, Q. Suna, Y. Wang, J. Tang and Y. Wang, A study on inhibition performance of mercaptoalcohols as corrosion inhibitors by first principle and molecular dynamics simulation, *Russ. J. Phys. Chem. A*, 2020, **94**, no. 9, 1877–1886. doi: 10.1134/S0036024420090356
5. Y. Qiang, L. Guo, H. Li and X. Lana, Fabrication of environmentally friendly Losartan potassium film for corrosion inhibition of mild steel in HCl medium, *Chem. Eng. J.*, 2021, **406**, 126863. doi: 10.1016/j.cej.2020.126863
6. G. Gece, Drugs: a review of promising novel corrosion inhibitors, *Corros. Sci.*, 2011, **53**, 3873–3898. doi: 10.1016/j.corsci.2011.08.006
7. A.S. Fouda, M.A. Ismail, A.M. Temraza and A.S. Abousalem, Comprehensive investigations on the action of cationic terthiophene and bithiophene as corrosion inhibitors: experimental and theoretical studies, *New J. Chem.*, 2019, **43**, 768–789. doi: 10.1039/C8NJ04330B
8. F. Touhami, A. Aouniti, Y. Abed, B. Hammouti, S. Kertit, A. Ramdani and K. Elkacemi, Corrosion inhibition of armco iron in 1 M HCl media by new bipyrazolic derivatives, *Corros. Sci.*, 2000, **42**, 929–940. doi: 10.1016/S0010-938X(99)00123-7
9. D. Chebabe, Z. Ait Chikh, N. Hajjaji, A. Srhiri and F. Zucchi, Corrosion inhibition of Armco iron in 1 M HCl solution by alkyltriazoles, *Corros. Sci.*, 2003, **45**, 309–320. doi: 10.1016/S0010-938X(02)00098-7
10. L.B. Furtado, R.C. Nascimento, P.R. Seidl, M.J.O.C. Guimarães, L.M. Costa, J.C. Rocha and J.A.C. Ponciano, Eco-friendly corrosion inhibitors based on Cashewnut shell liquid (CNSL) for acidizing fluids, *J. Mol. Liq.*, 2019, **284**, 393–404. doi: 10.1016/j.molliq.2019.02.083
11. L. Li, W. Xu, J. Lei, J. Wang, J. He, N. Li and F. Pan, Experimental and theoretical investigations of Michelia alba leaves extract as a green highly-effective corrosion inhibitor for different steel materials in acidic solution, *RSC Adv.*, 2015, **5**, 93724–93732. doi: 10.1039/C5RA19088F
12. S.A. Umoren, M.M. Solomon, I.B. Obot and R.K. Suleiman, A critical review on the recent studies on plant biomaterials as corrosion inhibitors for industrial metals, *J. Ind. Eng. Chem.*, 2019, **76**, 91–115. doi: 10.1016/j.jiec.2019.03.057

13. J.P. Vincken, L. Heng, A. Groot and H. Gruppen, Saponins, classification and occurrence in the plant kingdom, *Phytochem.*, 2007, **68**, 275–297. doi: 10.1016/j.phytochem.2006.10.008
14. S. Böttger and M.F. Melzig, Triterpenoid saponins of the *Caryophyllaceae* and *Illecebraceae* family, *Phytochem. Lett.*, 2011, **4**, 59–68. doi: 10.1016/j.phytol.2010.08.003
15. D. Kregiel, J. Berlowska, I. Witonska, H. Antolak, C. Proestos, M. Babic, L. Babic and B. Zhang, *Application and Characterization of Surfactants*, ed. R. Najjar, IntechOpen Limited, London, 2017.
16. A.N. Yücekutlu, S. Özbey and I. Bildacı, *Gypsophila simonii*: identification, extraction, isolation of sapogenin and X-ray crystallographic structure of sucrose, *Hacettepe J. Biol. Chem.*, 2012, **40**, 53–59.
17. G. Gece, The use of quantum chemical methods in corrosion inhibitor studies, *Corros. Sci.*, 2008, **50**, 2981–2992. doi: 10.1016/j.corsci.2008.08.043
18. A. Kokalj and D. Costa, *Encyclopedia of interfacial chemistry*, ed. K. Wandelt, Elsevier, Amsterdam, 2018, 332–345.
19. S. Sharma, X. Ko, Y. Kurapati, H. Singh and S. Nešić, Adsorption behavior of organic corrosion inhibitors on metal surfaces – some new insights from molecular simulations, *Corrosion*, 2019, **75**, 90–105. doi: 10.5006/2976
20. M.J. Frisch, G.W. Trucks, H.B. Schlegel, G.E. Scuseria, M.A. Robb, J.R. Cheeseman, G. Scalmani, V. Barone, G.A. Petersson, H. Nakatsuji, X. Li, M. Caricato, A. Marenich, J. Bloino, B.G. Janesko, R. Gomperts, B. Mennucci, H.P. Hratchian, J.V. Ortiz, A.F. Izmaylov, J.L. Sonnenberg, D. Williams-Young, F. Ding, F. Lipparini, F. Egidi, J. Goings, B. Peng, A. Petrone, T. Henderson, D. Ranasinghe, V.G. Zakrzewski, J. Gao, N. Rega, G. Zheng, W. Liang, M. Hada, M. Ehara, K. Toyota, R. Fukuda, J. Hasegawa, M. Ishida, T. Nakajima, Y. Honda, O. Kitao, H. Nakai, T. Vreven, K. Throssell, J.A. Montgomery, Jr., J.E. Peralta, F. Ogliaro, M. Bearpark, J.J. Heyd, E. Brothers, K.N. Kudin, V.N. Staroverov, T. Keith, R. Kobayashi, J. Normand, K. Raghavachari, A. Rendell, J.C. Burant, S.S. Iyengar, J. Tomasi, M. Cossi, J.M. Millam, M. Klene, C. Adamo, R. Cammi, J.W. Ochterski, R.L. Martin, K. Morokuma, O. Farkas, J.B. Foresman and D.J. Fox, *Gaussian 09*, *Revision C.01*, Gaussian, Inc., Wallingford CT, 2009.
21. R. Hasanzade, S. Bilgiç, G. Gece and Ö. Türkşen, Electrochemical and theoretical assessment of the effect of two biocides on the corrosion of petroleum steel in sulfur-polluted Black Sea water, *Mater. Corros.*, 2019, **70**, 2334–2342. doi: 10.1002/maco.201911072
22. A.V. Marenich, C.J. Cramer and D.G. Truhlar, Universal solvation model based on solute electron density and on a continuum model of the solvent defined by the bulk dielectric constant and atomic surface tensions, *J. Phys. Chem. B*, 2009, **113**, 6378–6396. doi: 10.1021/jp810292n

23. M. Stern and A.L. Geary, Electrochemical polarization. I. A theoretical analysis of the shape of polarization curves, *J. Electrochem. Soc*., 1957, **104**, 56–63.
24. J.O.M. Bockris and D. Drazic, The kinetics of deposition and dissolution of iron: effect of alloying impurities, *Electrochim. Acta*, 1962, **7**, 293–313.
25. G. Nechifor, D.E. Pascu, M. Pascu, G.A. Traistaru and P.C. Albu, Comparative study of Temkin and Flory-Huggins isotherms for adsorption of phosphate anion on membranes, *UPB Sci. Bull. Series B*, 2015, **77**, 63–72. ISSN: 1454-2331
26. N. Ayawei, A.N. Ebelegi and D. Wankasi, Modelling and interpretation of adsorption isotherms, *J. Chem*., 2017, 3039817. doi: 10.1155/2017/3039817
27. N. Labjar, F. Bentiss, M. Lebrini, C. Jama and S. El Hajjaji, Study of temperature effect on the corrosion inhibition of C38 carbon steel using amino-tris(methylenephosphonic) acid in hydrochloric acid solution, *Int. J. Corros*., 2011, Article ID 548528. doi: 10.1155/2011/548528
28. N.I. Kairi and J. Kassim, The effect of temperature on the corrosion inhibition of mild steel in 1 M HCl solution by *Curcuma Longa* extract, *Int. J. Electrochem. Sci*., 2013, **8**, 7138–7155.
29. A. Nahlé, I.I. Abu-Abdoun and I. Abdel-Rahman, Effect of temperature on the corrosion inhibition of trans-4-hydroxy-4′-stilbazole on mild steel in HCl solution, *Int. J. Corros*., 2012, 380329. doi: 10.1155/2012/380329
30. H. Khaleel, A.A. Ateeq and A.A. Ali, The effect of temperature and inhibitor on corrosion of carbon steel in acid solution under static study, *Int. J. Appl. Eng. Res*., 2018, **13**, 3638–3647. ISSN: 0973-4562
31. S. Satpati, S.K. Saha, A. Suhasaria, P. Banerjee and D. Sukul, Adsorption and anti-corrosion characteristics of vanillin Schiff bases on mild steel in 1 M HCl: experimental and theoretical study, *RSC Adv*., 2020, **10**, 9258–9273. doi: 10.1039/C9RA07982C
32. H.B. Michaelson, The work function of the elements and its periodicity, *J. Appl. Phys*., 1977, **48**, 4729–4733. doi: 10.1063/1.323539
33. Y.E. Kacimi, R. Touir, K. Alaoui, S. Kaya, A.S. Abousalem, M. Ouakki and M. Ebn Touhami, Anti-corrosion properties of 2-phenyl-4(3H)-quinazolinone-substituted compounds: electrochemical, quantum chemical, monte carlo, and molecular dynamic simulation investigation, *J. Bio. Tribo. Corros*., 2020, **6**, 47. doi: 10.1007/s40735-020-00342-1

♦♦♦